Developmental Biology **248,** 307–318 (2002)
doi:10.1006/dbio.2002.0711

Development Using Transgenic Zebrafish

Nathan D. Lawson and Brant M. Weinstein[1]

Laboratory of Molecular Genetics, NICHD, NIH, Building 6B, Room 309, 6 Center Drive, Bethesda, Maryland 20892

In this study we describe a model system that allows continuous *in vivo* observation of the vertebrate embryonic vasculature. We find that the zebrafish *fli1* promoter is able to drive expression of enhanced green fluorescent protein (EGFP) in all blood vessels throughout embryogenesis. We demonstrate the utility of vascular-specific transgenic zebrafish in conjunction with time-lapse multiphoton laser scanning microscopy by directly observing angiogenesis within the brain of developing embryos. Our images reveal that blood vessels undergoing active angiogenic growth display extensive filopodial activity and pathfinding behavior similar to that of neuronal growth cones. We further show, using the zebrafish *mindbomb* mutant as an example, that the expression of EGFP within developing blood vessels permits detailed analysis of vascular defects associated with genetic mutations. Thus, these transgenic lines allow detailed analysis of both wild type and mutant embryonic vasculature and, together with the ability to perform large scale forward-genetic screens in zebrafish, will facilitate identification of new mutants affecting vascular development.

Key Words: **angiogenesis; transgenics; vascular development; zebrafish.**

INTRODUCTION

The formation of a closed circulatory system in vertebrates is a complex process that involves a variety of signaling molecules and entails a diverse array of cellular behaviors (reviewed in Cleaver and Krieg, 1999). The blood vessels that make up the circulatory system are composed of a single endothelial cell layer surrounded by support cells, including pericytes, fibroblasts, and vascular smooth muscle cells (for example, see Gray, 1901). Endothelial precursor cells, or angioblasts, arise within the lateral mesoderm of vertebrate embryos (Sabin, 1920) and undergo two major processes, referred to as vasculogenesis and angiogenesis (Pardanaud *et al.*, 1989; Poole and Coffin, 1989), that lead to the formation of the primitive vascular network. Vasculogenesis describes the *de novo* formation of blood vessels through the coalescence of angioblasts (reviewed in Risau and Flamme, 1995). In contrast, angiogenesis involves the formation of new vessels from preexisting ones and is usually characterized by the sprouting of an endothelial cell from a previously formed vessel (reviewed in Wagner, 1980; Cleaver and Krieg, 1999). In addition to sprouting angiogenesis, vascular plexuses can be remodeled by intussusceptive angiogenesis leading to the establishment of an arborized and well-defined blood vessel structure (Djonov *et al.*, 2000). Although a great deal is known about the factors responsible for vasculogenesis and angiogenesis during embryonic development (reviewed in Cleaver and Krieg, 1999), there is little information concerning what governs the proper guidance of growing vessels and the cellular behaviors they display during these processes.

Many techniques have been utilized to observe endothelial cells and their precursors during embryogenesis. Early studies that led to the identification of blood and endothelial cell progenitor cells within the lateral mesoderm (Sabin, 1920) and initial observations on the mechanisms of angiogenesis (Clark, 1918) relied on light microscopy of live vertebrate embryos, while subsequent studies took advantage of electron microscopy (Hirakow and Hiruma, 1981; Meier, 1980) to observe these processes. These observations were later refined by immunostaining using antibodies specific to primitive hematopoietic and vascular precursors (Coffin and Poole, 1988; Pardanaud *et al.*, 1987) and contributed to the definition of vasculogenic and angiogenic blood vessel growth (Poole and Coffin, 1989). The patent vasculature of vertebrate embryos can also be visualized by injecting dyes (for example, see Latker *et al.*, 1986), or

[1] To whom correspondence should be addressed. Fax: (301) 435-6001. E-mail: bw96w@nih.gov.

0012-1606/02 $35.00

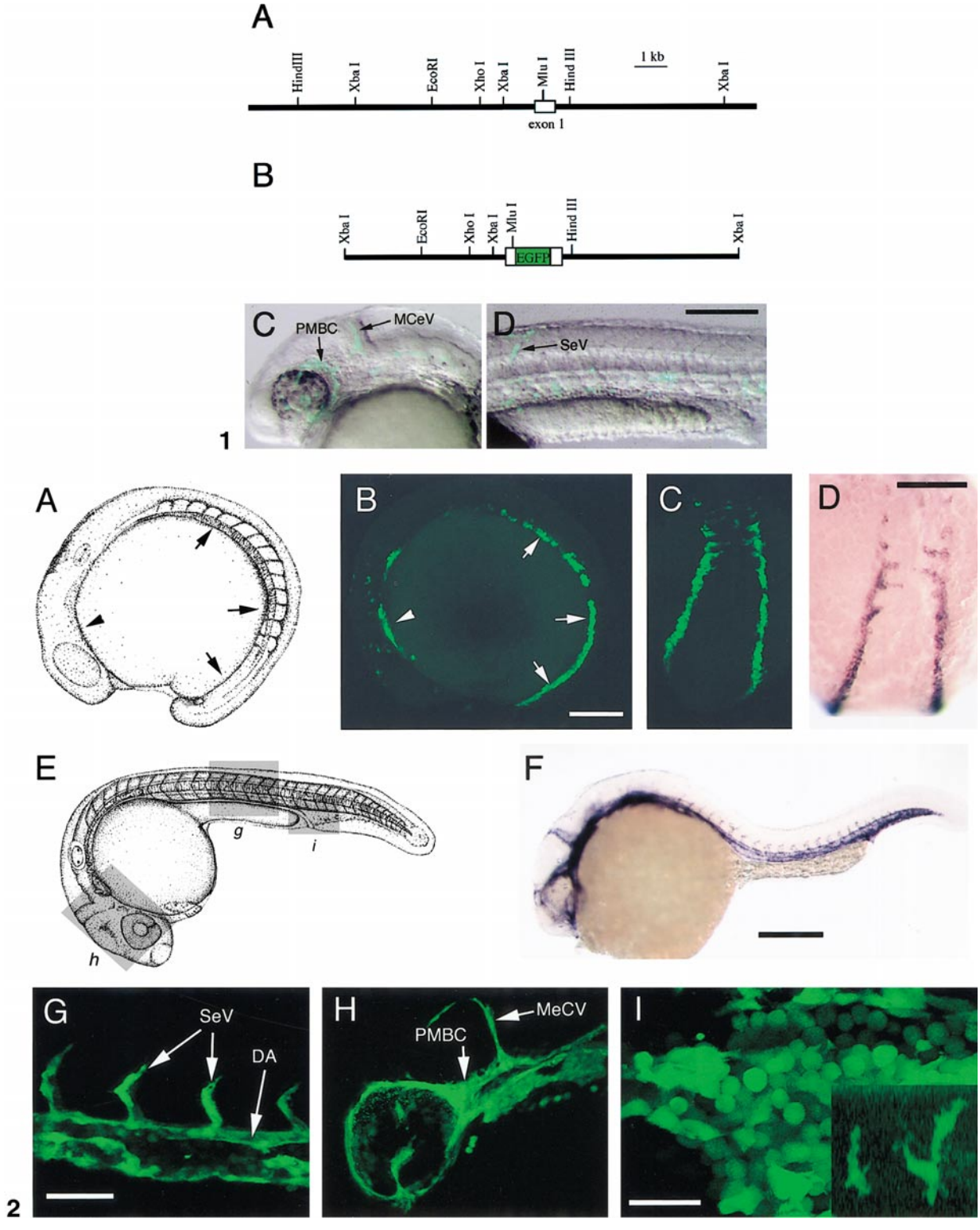

FIG. 1. Structure of *fli1* 5′ genomic region and injection construct. (A) Restriction map of the genomic region surrounding the first exon of zebrafish *fli1*. (B) Restriction map of the *fli1* genomic fragment and EGFP transgene in the pfli15EGFP construct used for injection and establishment of transgenic lines. (C, D) Merged transmitted light and fluorescent images of live embryos injected with linearized pfli15EGFP at 26 hpf; lateral views, anterior is to the left, dorsal is up. (C) EGFP expression within the primordial midbrain channel (PBMC) and midcerebral vein (MCeV) in the head of an injected embryo. (D) EGFP expression in a segmental vessel (SeV). Scale bar, 200 μm.

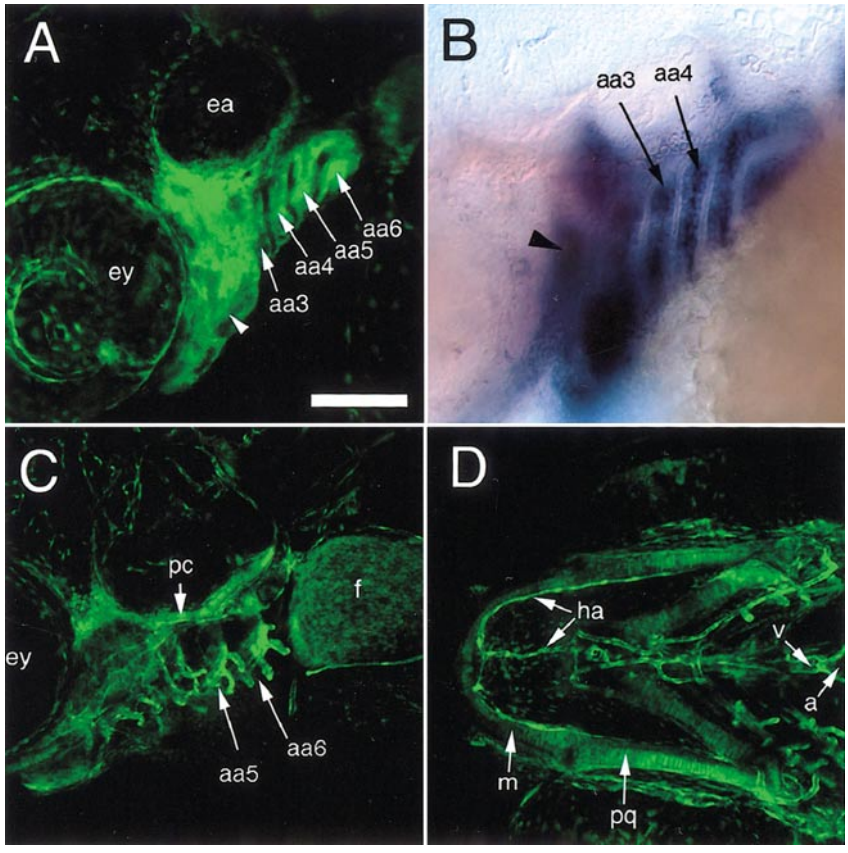

FIG. 3. EGFP expression in cranial neural crest derivatives in *TG(fli1:EGFP)*^{y1}*; alb*^{b4} embryos. (A–C) Lateral views, anterior is to the left, dorsal is up. (A) Live 2-dpf embryo expressing EGFP within the aortic arches (aa3–6aa, arrows) and the mesenchyme of the forming jaw (arrowhead); ey, eye; ea, ear. (B) Whole-mount *in situ* hybridization of endogenous *fli1* transcript showing expression within aortic arches (arrows) and jaw primordium (arrowhead, out of focal plane). (C) Live 7-dpf larva showing EGFP expression in structures such as the parachordal cartilage (pc) as well as the vessels within the gills arches (aa5 and aa6; white arrow). EGFP expression is also apparent in the mesenchyme of the developing fin bud (f). (D) Ventral view of embryo in (C); EGFP expression in cells of the forming the jaw, such as Meckel's cartilage (m) and the palatoquadrate (pq), and associated vessels, such as the hypobranchial artery (ha) as well as the ventricle (v) and atrium (a) of the heart. Scale bar, 100 μm.

fluorescently labeled compounds (Nilsen, 1981), into the circulation. For example, we have injected fluorescent microspheres into the circulation of zebrafish embryos followed by confocal laser microscopy to characterize wild type or mutant circulatory networks at various time points (Isogai *et al.*, 2001; Weinstein *et al.*, 1995). However, there

FIG. 2. EGFP expression in live *TG(fli1:EGFP)*^{y1} embryos. (A) Camera lucida drawing (modified from Kimmel *et al.*, 1995) of a zebrafish embryo at 14 hpf. Arrowhead indicates region of anterior lateral mesoderm and arrows indicate posterior lateral mesoderm shown in (B). (B) Expression of EGFP within the anterior (arrowhead) and posterior (arrows) lateral mesoderm of a 12-somite-stage *TG(fli1:EGFP)*^{y1} embryo; lateral view, anterior is to the left. (C) Dorsal view of posterior lateral mesoderm in the embryo shown in (B). (D) Dorsal view of 12-somite-stage embryo stained by *in situ* hybridization with Fli1; same view as (C). (E) Camera lucida drawing (modified from Kimmel *et al.*, 1995) of a zebrafish embryo at 24 hpf. Boxed regions indicate views in (G–I). (F) Lateral view of 24-hpf embryo stained for *in situ* hybridization with Fli1; same view as (E). (G–I) Lateral views, anterior is to the left, dorsal is up; images obtained using mulitphoton laser microscopy. (G) EGFP expression in trunk vessels at 24 hpf, including the dorsal aorta (DA) and segmental vessels (SeV). (H) EGFP expression in the major vessels of the head of a *TG(fli1:EGFP)*^{y1} embryo at 24 hpf; midcerebral vein (MCeV) and primordial midbrain channel (PMBC) are indicated. (I) EGFP expression in primitive erythroid progenitors within the caudal vein of a 24-hpf *TG(fli1:EGFP)*^{y1} embryo and cells with macrophage morphology on the yolk sac (inset). Scale bar, (B, C, D, F) 200 μm; (G, H) 50 μm; (I) 25 μm.

are significant drawbacks to many of these analyses. The most commonly used methods for visualizing cells and tissues *in situ* require fixation or are otherwise limited to visualization at only a single time point. Microangiography is performed on live embryos, but this technique does not allow the observation of actively growing vessels that are unable to carry flow, thus hindering analysis of early vasculogenic processes and initial angiogenic sprouting. Therefore, it would be beneficial to devise a system that allows prolonged *in vivo* imaging of endothelial cell behavior at any stage of development in a noninvasive manner.

The transparency and external development of the zebrafish embryo and the ability to produce tissue-specific germ line transgenic fish expressing enhanced green fluorescent protein (EGFP; reviewed in Lin, 2000) make this organism an ideal system with which to visualize the formation of the embryonic vasculature. Therefore, we have established transgenic zebrafish expressing EGFP driven by the promoter for *fli1,* a known endothelial cell marker in mouse (Melet *et al.,* 1996), which is also expressed during vascular development in zebrafish embryos (Thompson *et al.,* 1998). We find that a 15-kb genomic fragment encompassing the zebrafish *fli1* first exon is sufficient to drive expression within the blood vessels of embryos derived from germline founders. EGFP is detected in the lateral mesoderm during early somitogenesis and expression persists within all blood vessels through at least 7 days postfertilization (dpf). Transgene expression is also found in hematopoietic cell types and jaw mesenchyme. Using multiphoton laser scanning microscopy of transgenic embryos, we are able to perform time-lapse imaging of embryonic angiogenesis during vascularization in the developing zebrafish brain. Our observations reveal that angiogenic blood vessels have similarities to nerve growth cones, including dynamic filopodial activity and pathfinding behaviors. Finally, we show the utility of these vascular specific transgenic lines in the analysis of mutant vascular patterning by observing blood vessel structure and patterning in the zebrafish mutant, *mindbomb*.

MATERIALS AND METHODS

Zebrafish

Zebrafish (*Danio rerio*) embryos used for injections were obtained from natural spawnings of a wild type EK line. This line was obtained from Ekkwill Farms (Gibonston, FL) and has been inbred for several generations. The *albino* (*alb*^{b4}; Streisinger *et al.,* 1986) and *mindbomb* (*mib*^{ta52b}; Jiang *et al.,* 1996) lines have been described previously. Embryos and fish from all lines were raised and maintained as described (Westerfield, 1993). Generation and characterization of the *TG(fli1:EGFP)* lines are described in this paper. The *TG(fli1:EGFP)*^{y1} and *TG(fli1:EGFP)*^{y5} lines are available through the Zebrafish International Resource Center (Eugene, OR; http://zfin.org/zf_info/stckctr/submission/request.html).

Generation of Constructs and Transgenic Lines

Fragments spanning the 5′ end of the *fli1* gene were obtained by screening a PAC library by hybridization to a fragment of the *fli1* 5′ UTR. PAC DNA was digested with *Xba*I and subcloned into pGEM3zf (Promega, Madison, WI). Both *Xba*I fragments were cloned into a contiguous orientation, and EGFP was placed just upstream of the *fli1* start codon to give the plasmid pfli15EGFP. A detailed description of the cloning of this construct is available on request. Prior to injection, pfli15EGFP was linearized with *Not*I, extracted once with phenol:chloroform and once with chloroform, and ethanol precipitated. Linearized DNA was resuspended in nuclease-free water. Approximately 200–300 pg of linearized DNA was injected into one-cell-stage embryos no later than 20 min following fertilization by using standard protocols (Xu, 1999). The following day, fluorescence was monitored by using a Leica dissection scope equipped with epifluorescence (MZFLII). Only embryos displaying fluorescence were grown to adulthood. Pairs of sibling adults grown from injected embryos were incrossed to identify germ line founders. Subsequently, individual adults from positive pairs were outcrossed to identify the individual founder fish.

Microscopic Imaging

Embryos were dechorionated manually with watchmakers' forceps and held in 30% Danieu's buffer for imaging. For later time points, embryos were anesthetized by placing in 30% Danieau's containing 0.003% tricaine methanesulfonate (Sigma, St. Louis, MO). 1-Phenyl-2-thiourea (0.002%) was also added when nonalbino embryos were imaged in order to prevent pigment development. For collection of single time points, embryos were mounted in 5% methylcellulose (Sigma) dissolved in 30% Danieau's buffer. For time-lapse imaging, embryos were held by partially embedding them in low-melt agarose immersed in 30% Danieu's buffer in a chamber prepared from a modified 60-mm petri dish. Imaging was performed with 40× or 60× water immersion objectives. Embryos held in this way maintained heartbeat and robust circulation throughout the imaging period.

Confocal and multiphoton laser scanning microscopy was performed by using a Radiance 2000 Imaging System (BioRad, Hercules, CA). Except where indicated, images at single time points were obtained by using standard confocal microscopy with a krypton–Argon laser at 480 nm. For time-lapse analysis, multiphoton imaging was performed by using 950-nm pulsed-mode-locked laser emission from a Tsunami tunable Ti-Sapphire laser (Spectra Physics Lasers, Inc., Mountain View, CA). Time-lapse imaging was performed with the minimal necessary laser power. Stacks of frame-averaged (3–5 frames) sections were collected digitally and reconstructed by using the Metamorph software package (Universal Imaging Corp., Downingtown, PA). Data on the frame intervals, total duration, number of Z-sections, and spacing between Z-section planes for each of the time-lapse movies are provided at http://zfish.nichd.nih.gov/zfatlas/fli-gfp/Fli_Movies.html.

In Situ Hybridization

Whole-mount *in situ* hybridization was performed as described elsewhere (Hauptmann and Gerster, 1994) by using a probe for *fli1* (Thompson *et al.,* 1998). Images were acquired by using a Zeiss Axiophot2 equipped with a ProgRes mF digital camera (Jenoptik, Eching, Germany).

TABLE 1
Comparison of Copy Number and Expression Level in *TG(fli1:EGFP)* Founders

Founder adult	Allele name	Copy number	Expression level	Expression pattern
A	*y1*	>25	++++	bv, bc, nc
C	*y2*	7	+++	bv, bc, nc
D	*y3*	2	+	bv, bc, nc
E	*y4*	1	+	bv, bc, nc
F	*y5*	4.5	+++	bv, bc, nc

Note. Copy number was determined by Southern analysis. Expression level was determined by qualitative observation at 24 hpf using a dissection microscope equipped with epifluorescence. bv, blood vessels; bc, blood cells; nc, neural crest derivatives.

RESULTS

Establishment of TG(fli1:EGFP) Germline Transgenic Zebrafish

We chose to use the promoter for *fli1* to drive EGFP expression in transgenic lines since it is the earliest known endothelial cell marker in zebrafish and persists in blood vessels until at least 2 dpf (Thompson *et al.*, 1998). Two *Xba*I fragments were found that span approximately 15 kb of the putative *fli1* promoter and include exon 1 (Fig. 1A). EGFP was cloned into the 5′ UTR just upstream of the *fli1* start codon, and these fragments were placed contiguously into pGEM3zf (Fig. 1B). Injection of this construct (referred to as pfli15EGFP) into one-cell-stage zebrafish embryos results in mosaic EGFP expression within blood vessels of the head, such as the primordial midbrain channel and midcerebral vein (Fig. 1C), as well as the trunk, such as the segmental vessels (Fig. 1D), at 26 h postfertilization (hpf).

To establish stable transgenic lines, one-cell-stage embryos were injected with linearized pfli15EGFP and grown to adulthood. From 142 adults grown from injected embryos, 21 founders were identified. Most of these founder fish produced embryos that expressed EGFP at levels barely detectable using a dissecting microscope equipped with epifluorescence (data not shown). Embryos from 5 different founder fish that exhibited higher levels of EGFP expression were maintained and analyzed in subsequent generations. The lines have been assigned names according to standard zebrafish nomenclature and are hereafter referred to as *TG(fli1:EGFP)* with allele designations *y1* through *y5*. All 5 lines display the same temporal and spatial pattern of EGFP expression and exhibit Mendelian inheritance of the transgene (data not shown), indicating that that the injected DNA integrated at single loci. We find that the lines differ in the level of EGFP expression which correlates with transgene copy number as determined by Southern analysis (Table 1).

EGFP expression pattern in TG(fli1:EGFP) embryos

To characterize the expression pattern of EGFP in *TG(fli1:EGFP)* lines, we utilized confocal laser scanning microscopy. The *TG(fli1:EGFP)^{y1}* line was used to obtain the images for the following figures. Expression can be detected at low levels as early as the three-somite stage within the posterior lateral mesoderm (data not shown; endogenous *fli1* transcript is also first detectable by *in situ* hybridization at about this time; Thompson *et al.*, 1998) and continues to be expressed throughout somitogenesis within the anterior and posterior lateral mesoderm (Figs. 2B and 2C), in patterns indistinguishable from the endogenous *fli1* transcript (Fig. 2D). At 24 hpf, the pattern of endogenous *fli1* transcript is also indistinguishable from that of EGFP in trasngenics. Major trunk vessels, such as the dorsal aorta, are apparent in *TG(fli1:EGFP)^{y1}* embryos, as are segmental vessels sprouting from the dorsal aorta (Fig. 2G). The primordial midbrain channel and midcerebral vein are visible within the head at this time (Fig 2H). We can also detect EGFP expression in hematopoietic cells in *TG(fli1:EGFP)^{y1}* embryos. EGFP-positive cells with erythroid morphology are apparent at 24 hpf (Fig. 2I), but are not found in circulation at 3 dpf (see Movie 1; movies can be accessed at http://zfish.nichd.nih.gov/zfatlas/fli-gfp/Fli_Home.html). A small percentage of circulating cells at 3 dpf express EGFP at high levels and occasionally adhere to and roll within the blood vessels (see Movie 1). EGFP is also expressed in cells with macrophage morphology that are found on the yolk sac (Fig. 2I, inset) and elsewhere throughout the embryo (data not shown).

In several vertebrate species, including zebrafish, *fli1* is expressed in derivatives of cranial neural crest, such as the mesenchyme of the aortic arches and the developing cartilage of the jaw (Mager *et al.*, 1998; Meyer *et al.*, 1993; Thompson *et al.*, 1998). Therefore, we determined if *TG(fli1:EGFP)* lines exhibited a similar pattern of EGFP expression. At 2 dpf, we can detect EGFP within the aortic arches as well as the developing jaw (Fig. 3A) identical to the expression of endogenous *fli1* transcript (Fig. 3B). EGFP expression in these neural crest derivatives persists until at least 7 dpf, allowing detailed visualization of the forming gill arches (Figs. 3C) and jaw cartilage (Figs. 3C and 3D) as well as the vasculature that is in close proximity to these structures, such as the hypobranchial artery (Fig. 3D). Expression is also noted in the developing fin mesenchyme

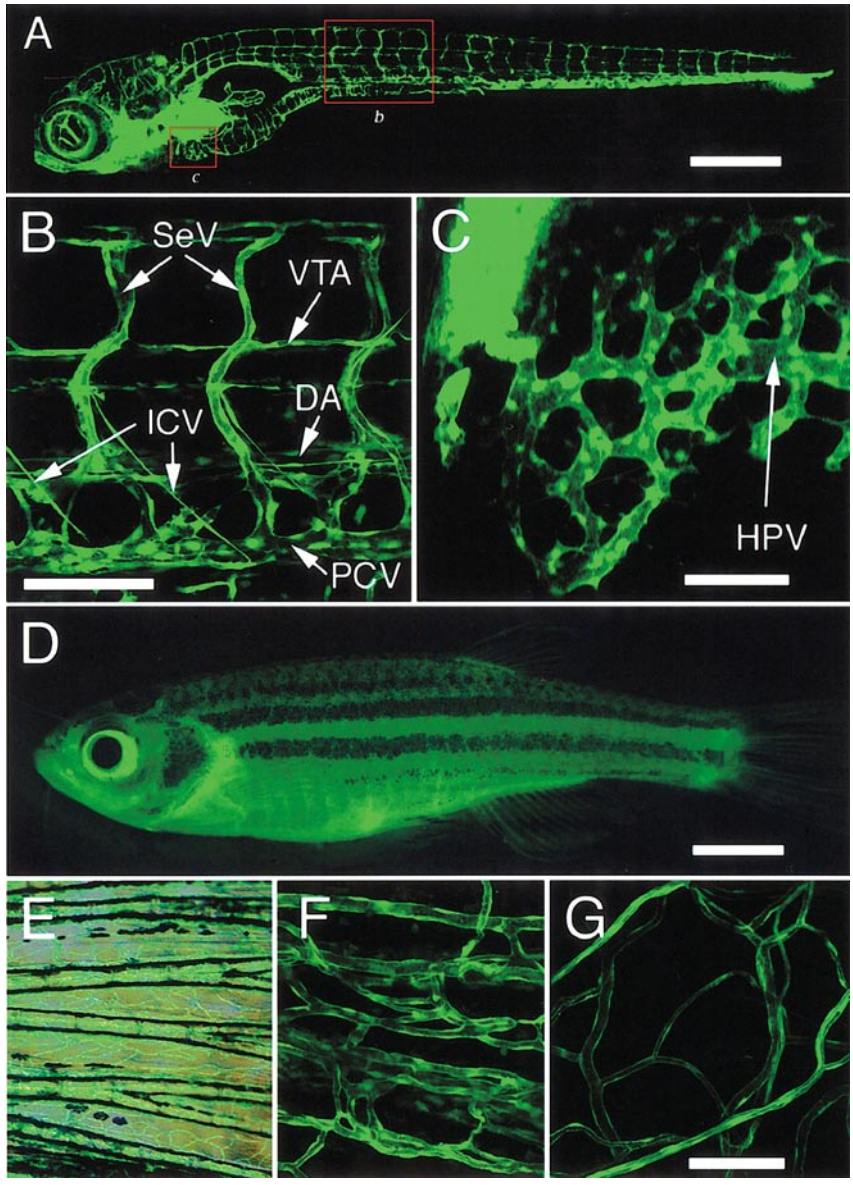

FIG. 4. EGFP expression in the vasculature of live *TG(fli1:EGFP)*^{y1}; *alb*^{b4} larvae and adults. (A–G) Lateral views, anterior to the left, dorsal is up. (B, C, F, G) Images acquired using multiphoton laser scanning microscopy. (A) A 7-dpf larva, compiled from five separate image reconstructions. Boxed areas labeled "b" and "c" indicate regions shown in (B) and (C), respectively; images in (A) and (B) are from two different larvae. (B) Image of trunk vessels at 7 dpf showing patent vessels such as the dorsal aorta (DA), posterior cardinal vein (PCV), segmental vessels (SeV), as well as vessels that do not carry blood flow at this time such as the vertebral arteries (VTA) and intercosta vessels (ICV). (C) Hepatic (liver) vasculature in a 5-dpf larva. The hepatic portal vein (HPV) is noted (arrow). (D) Full-length view of *TG(fli1:EGFP)*^{y1} adult fish. (E) Merged transmitted light and fluorescent image from the tail fin of the fish shown in (D). (F) Tail fin microvasculature in adult shown in (D). (G) EGFP-positive blood vessels associated with surface scales in adult shown in (D). Three-dimensional reconstructions of the images in (B), (C), (F), and (G) are available at http://zfish.nichd.nih.gov/zfatlas/fli-gfp/Fli_Home.html. Scale bar, (A) 500 μm; (B) 100 μm; (C) 50 μm; (D) 5 mm; (F, G) 100 μm.

(Fig. 3C). Expression of EGFP in all blood vessels persists until at least 7 dpf (Figs. 4A–4C), at which time it is possible to visualize the vasculature of developing organs, such as the liver (Fig. 4C) and brain (see below). EGFP expression can also be detected in adult transgenic fish (Fig. 4D), for example, within the microvasculature of the fins (Figs. 4E and 4F) and individual scales on the body surface (Fig. 4G).

Time Lapse Imaging of Vascularization in the Zebrafish Brain

To assess the utility of the *TG(fli1:EGFP)* lines for studying the development of embryonic blood vessels *in vivo*, we performed time-lapse multiphoton laser scanning microscopy to observe vascularization within the developing brain of the zebrafish embryo. Microangiography only allows visualization of patent, functioning blood vessels, and most growing angiogenic vessels are not initially patent, or even lumenized. At 3 dpf, central arteries can be visualized within the hindbrain of *TG(fli1:EGFP)*^{y1} embryos (Fig. 5A; three-dimensional reconstructions and time-lapse movies are available at http://zfish.nichd.nih.gov/zfatlas/fli-gfp/Fli_Home.html). The growing vessel sprouts appear extremely dynamic, extending and retracting long filopodial processes in successive frames of our time-lapse sequences (Fig. 5B; for example, compare time points 210′ and 240′; and Movie 2). Growing central arteries also display repulsion and pathfinding behavior. For example, the central artery sprout in Fig. 5D approaches a lumenized vessel (time point 135′), comes in contact with it via filopodial extensions (Fig. 5D, 255′), and then turns and begins growing in a different direction (Fig. 5D, time points 300′ and 450′; see also Movie 4). Vascular remodeling and regression are also readily apparent in time-lapse analyses of forming central arteries. For example, a connection between adjacent vessels that is not patent is lost while nearby another connection strengthens and becomes patent (Fig. 5C; and see Movie 3).

We are also able to visualize the sequence of pathfinding and contact between an angiogenic sprout to its target vessel. In this case, we observed the growth of the communicating vessel and its contact with its target vessel, the palatocerebral artery within the 2-dpf forebrain (Fig. 5E; see Isogai *et al.*, 2001). Like the vessels in the hindbrain, the growing communicating vessel also exhibits extensive filopodial activity (Fig. 5F, 255′–390′; and Movie 5). We find that the palatocerebral artery also displays similar filopodial extensions and appears to itself initiate a sprout in the direction of the approaching communicating vessel (Fig. 5F, 315′; and see Movie 5). However, this sprout regresses on contact between the communicating vessel and the palatocerebral artery (Fig. 5F; compare 315′ and 390′; see Movie 5). In addition, the filopodial activity of the communicating vessel and its target vessel ceases once the connection between these vessels is made (Fig. 5F, compare 390′ and 480′ time points), but just before lumenization of the communicating vessel is apparent (Movie 5). Note that this sequence shows the growth of only the left communicating vessel. In this embryo, the right communicating vessel only began to extend once the left communicating vessel was already patent.

Since the expression of EGFP is first detectable beginning at about the three-somite stage, the *TG(fli1:EGFP)* lines are also very useful for studying the initial formation of blood vessels by vasculogenesis during early embryogenesis. We used time-lapse imaging to examine angioblast migration during vasculogenesis of the primary axial vessels of the zebrafish trunk, the dorsal aorta, and posterior cardinal vein (Movie 6). Individual angioblasts can be seen exiting the strip of lateral mesodermal EGFP-positive cells and actively migrating in towards the trunk midline. The remaining more lateral cells also slowly migrate as a cohort toward the trunk midline.

Visualizing Vascular Abnormalities in mindbomb Mutant Embryos

We have previously noted defects in segmental vessel patterning and severe cranial hemorrhage associated with loss of Notch signaling in zebrafish embryos mutant for the *mindbomb* (*mib*) locus (Lawson *et al.*, 2001). However, microangiography analysis of head vessels in *mib* mutant embryos is often complicated by lack of circulation and severe cranial hemorrhage that leads to excessive leakage of fluorescent microspheres (N.D.L., unpublished observations). Furthermore, this technique does not allow analysis of earlier steps during segmental vessel formation. By crossing *mib*^{ta52b} carriers into the *TG(fli1:EGFP)* background, we are able to directly visualize the vessels in *mib*^{ta52b} embryos carrying the *fli1*:EGFP transgene, obviating the need for microangiography.

In an effort to determine the nature of cranial hemorrhage due to loss of *mib*, we observed the structure of head vessels in *TG(fli1:EGFP)*^{y1}; *mib*^{ta52b} mutant embryos at 2 dpf. In wild type *TG(fli1:EGFP)*^{y1} embryos, a clearly defined vascular structure can be seen within the hindbrain (Fig. 6A, region posterior to the midcerebral vein) with the midcerebral vein apparent at its normal position along the midbrain–hindbrain boundary (see Isogai *et al.*, 2001). *TG(fli1:EGFP)*^{y1} embryos mutant for *mib*^{ta52} exhibit massive disorganization of the vessels within the hindbrain, with no definable stereotypic structure evident (Fig. 6B). However, the location and pattern of the midcerebral vein appear normal in mutant embryos (Fig. 6B), although significant dilation of this vessel is evident when compared with wild type siblings (Fig. 6A).

As mentioned above, *mib*^{ta52b} mutant embryos display defects in segmental vessel patterning at 2 dpf. Wild type *TG(fli1:EGFP)*^{y1} embryos display segmental vessels at regular intervals along the vertical myosepta of the somites (Fig. 6C), while *TG(fli1:EGFP)*^{y1}; *mib*^{ta52b} mutant embryos display ectopic segmental vessel sprouts that enter the somitic tissue (Fig. 6D). To determine whether earlier defects were apparent during the initial sprouting of the segmental vessels, we observed these vessels at the 20-somite stage in *TG(fli1:EGFP)*^{y1} embryos. The lack of a patent circulatory system at this time point precludes the use of microangiography, but nascent segmental vessel sprouts are easily visualized in *TG(fli1:EGFP)*^{y1} embryos. Segmental vessels sprouts can be seen emanating from the dorsal aorta at each vertical myoseptum in 20-somite-stage wild type *TG(fli1:EGFP)*^{y1} embryos (Fig. 6E; and data not shown). Similar to

wild type embryos, segmental vessel sprouts in *TG(fli1:EGFP)^{y1}*; *mib^{ta52b}* mutant embryos are also only found at the vertical myosepta at the 20-somite stage (Fig. 6F)

DISCUSSION

In this study we describe the establishment of transgenic zebrafish expressing EGFP driven by the *fli1* promoter. We find that a 15-kb fragment of the zebrafish *fli1* promoter is sufficient to recapitulate the known expression pattern of the endogenous *fli1* transcript (Thompson *et al.*, 1998) until at least 2 dpf. EGFP is expressed in all blood vessels in *TG(fli1:EGFP)* embryos and larvae, at all stages of development assayed, and can be detected within the microvasculature of adult fish. During embryonic development, EGFP expression is detected in both patent and forming blood vessels, as well as in migratory angioblasts that have not yet aggregated into vascular structures. In this respect these transgenic lines provide a major advantage for visualizing the development of blood vessels over other methods, such as confocal microangiography (Weinstein *et al.*, 1995), which only permit observation of patent vessels effectively connected to the circulatory network. In addition, EGFP can be viewed for extended periods in live embryos, allowing continuous observation of blood vessel development as it occurs. Previous studies have described vascular-specific EGFP expression in transgenic zebrafish embryos by using the mouse *tie2* promoter (Motoike *et al.*, 2000). However, these embryos exhibit ectopic hindbrain and neural tube expression precluding visualization of blood vessels within the head and do not express sufficient levels of EGFP to allow them to be used for effective long-term imaging or as a screening tool (N.D.L., unpublished observation). In contrast, blood vessel structure in *TG(fli1:EGFP)^{y1}* embryos is easily viewed with the aid of a dissection microscope equipped with epifluoresence, enabling rapid screening of abnormal patterning associated with a mutant phenotype.

TG(fli1:EGFP) embryos also express EGFP in the mesenchyme and cartilage of the developing jaw, consistent with endogenous *fli1* expression in zebrafish (Thompson *et al.*, 1998). We have also observed EGFP expression in hematopoietic cells in *TG(fli1:EGFP)* embryos. EGFP-positive erythroid cells are present at 24 hpf, and we have noted low-level expression of *fli1* transcript in these same cells (N.D.L., unpublished observation). However, erythroid expression appears to be downregulated as development proceeds and we are able to detect EGFP only in a small proportion of circulating cells at 3 dpf. The occasional adhesive and rolling behavior of these cells suggests that they may be circulating myeloid cells, although we cannot rule out the possibility that they are megakaryocytes which are known to express *fli1* in mouse (Melet *et al.*, 1996) and can exhibit attachment to endothelial cells (Avraham *et al.*, 1993). EGFP expression is also apparent in cells on the surface of the yolk sac. These cells exhibit macrophage morphology and their location is consistent with previous studies describing macrophages in zebrafish embryos (Herbomel *et al.*, 1999).

Time Lapse Imaging of Embryonic Blood Vessels

TG(fli1:EGFP) embryos provide an excellent opportunity for visualizing blood vessel development as it occurs *in vivo*. However, the continuous use of confocal laser scanning microscopy for long periods during time-lapse imaging

FIG. 5. Time-lapse analyses of cranial vessels in *TG(fli1:EGFP)^{y1}; alb$^{b4/b4}$* larvae using multiphoton imaging. (A) Central arteries in zebrafish hindbrain at approximately 3.5 dpf, dorsal view, anterior to the right; see (G) for orientation of images. (B–D) Time-lapse sequences of the regions delineated by the corresponding boxes (b, c, d) in (A). (B) A growing central artery exhibiting extension and regression of numerous filopodial extensions (arrows in 210′ and 240′; see Movie 2). (C) A branched central artery exhibits regression of one connection (indicated by an arrow throughout the sequence), while the other connection is retained and appears lumenized by the end of the sequence (arrowhead; see Movie 3). (D) A central artery sprout (arrowhead in time points 135′ and 255′) contacts a potential target vessel via its numerous filopodia. It then regresses and sprouts in a different direction (arrow, time points 255′ and 450′; see Movie 4). (E) Zebrafish forebrain at approximately 2.5 dpf showing communicating vessel (arrow) and palatocerebral artery (arrowhead), frontal view, dorsal up; see (G) for orientation. Brightly labeled plexuses of vessels behind the eye are noted (asterisks). Boxes indicate contact with the palatocerebral artery. Both the communicating vessel and palatocerebral artery exhibit filopodial extensions on the surface (for example, see time point 255′). Filopodial activity in both vessels diminishes just prior to lumenization of the communicating vessel (compare time points 315′ and 480′; see Movie 5). Time-lapse movies and selected three-dimensional reconstructions are available at http://zfish.nichd.nih.gov/zfatlas/fli-gfp/Fli_Home.html. Scale bar, (A, E) 50 μm.

FIG. 6. Vascular defects in *TG(fli1:EGFP)^{y1}; mib^{ta52b}* embryos. (A) Head of a wild type *TG(fli1:EGFP)^{y1}* embryo at 2 dpf. Arrow indicates midcerebral vein which runs along the midbrain–hindrain boundary. (B) Head vasculature within the hindbrain (posterior to the midcerebral vein) of a *TG(fli1:EGFP)^{y1}; mib^{ta52b}* mutant embryo is severely disorganized and highly dilated. The location and pattern of the midcerebral vein appears normal, although it appears dilated. (A, B) Dorsal views, anterior is to the left. (C) Segmental vessels (arrows) appear at regular intervals corresponding to the vertical myosepta of the somites in a wild type *TG(fli1:EGFP)^{y1}* embryo. (D) In *TG(fli1:EGFP)^{y1}* embryos mutant for *mib^{ta52b}*, ectopic segmental vessel sprouts (arrowheads) are seen throughout the trunk. (E) A wild type sibling *TG(fli1:EGFP)^{y1}* at the 20-somite stage with segmental vessels (arrows) sprouting from the dorsal aorta. (F) Segmental vessel sprouts appear normal in*TG(fli1:EGFP)^{y1}; mib^{ta52b}* mutant embryos at the 20-somite stage. (C–F) Lateral views, anterior is to the left, dorsal is up. Scale bar, (C–F) 50 μm.

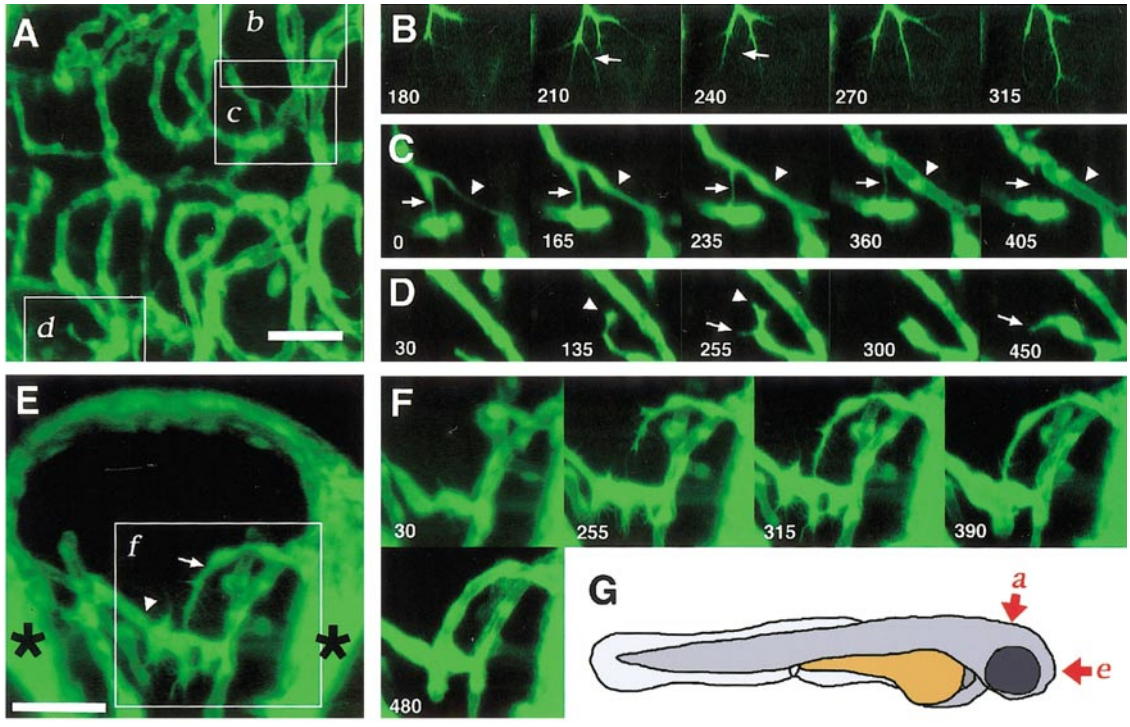

5

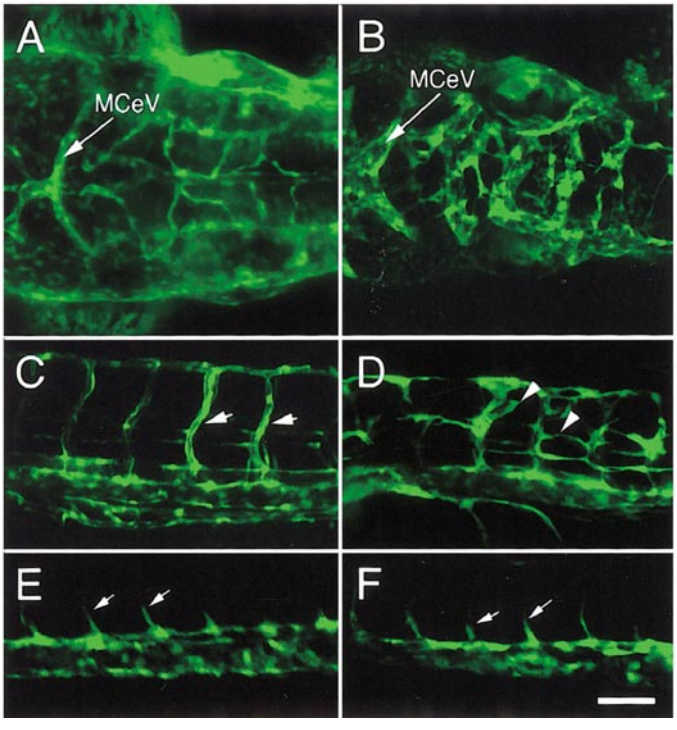

6

can damage target tissue leading to aberrant development of the area of interest. Therefore, we performed time-lapse imaging using multiphoton laser scanning microscopy, which provides better optical sectioning and penetration while causing less damage to the target area (reviewed in Denk and Svoboda, 1997). We have not noted aberrant or delayed development within vessels imaged in this study, and we have successfully performed imaging for up to 24 h with no effects on the development or viability of the embryos (B.M.W., unpublished observations). Time-lapse analysis of vascularization in *TG(fli1:EGFP)*^{y1} embryos reveals that angiogenic blood vessel sprouts bear striking resemblance in appearance and behavior to axonal growth cones (Bray and Chapman, 1985). Similar growth cone-like filopodial extensions on embryonic endothelial cells have been documented during vascularization of the cerebral cortex in hamsters (Marin-Padilla, 1985) and have long been known to be a characteristic of angiogenic blood vessels (reviewed in Cleaver and Krieg, 1999; Wagner, 1980) although their function remains unknown. In this study we are able to visualize the behavior of these dynamic structures *in vivo* during normal vascular development in *TG(fli1:EGFP)*^{y1} embryos.

We observe that both sprouting vessels and their vascular targets display filopodia on their surfaces, suggesting that this activity is initiated on both vessels by local cues within the surrounding tissue. Subsequent downregulation of filopodial activity occurs soon after contact with the target vessel and appears to be closely linked to morphogenesis of the sprouting vessel. During growth of sprouting vessels, filopodial extensions appear to properly target the growing vessel to the correct location, similar to their proposed function in axon growth cones (Chien *et al.*, 1993). As in axonal pathfinding, proper targeting of blood vessels appears to be mediated by both attractive and repulsive interactions with potential vascular targets and other surrounding tissues. Given their morphologic and behavioral similarities, it is likely that molecules known to play roles in axon pathfinding, such as members of the ephrin family of transmembrane ligands and their Eph receptors (reviewed in Zhou, 1998), mediate some of these interactions. Endothelial cells are known to express several members of these families (Gerety *et al.*, 1999; Wang *et al.*, 1998) and disruption of ephrin–Eph signaling in vertebrate embryos leads to defects in patterning of some vessels formed by sprouting angiogenesis, such as the intersomitic arteries and veins (Adams *et al.*, 1999; Gerety *et al.*, 1999; Helbling *et al.*, 2000; Wang *et al.*, 1998). In addition, we have also noted loss of *ephrin-B2a* expression within the blood vessels of *mib*^{ta52b} mutant embryos (Lawson *et al.*, 2001), which display segmental vessel pathfinding defects (see below).

Analysis of a Mutant Vascular Phenotype in TG(fli1:EGFP); mib^{ta52b} *Embryos*

Previous work from our laboratory has shown that loss of Notch signaling in *mib*^{ta52b} mutant embryos results in a variety of vascular defects associated with disruption of proper arterial–venous identity (Lawson *et al.*, 2001). Consistent with our previous observations, we find that the segmental vessels display ectopic sprouting within the somites in *TG(fli1:EGFP)*^{y1}; *mib*^{ta52b} mutant embryos. Furthermore, the presence of the EGFP transgene allows us to observe that the initial sprouting of segmental vessels at the vertical myosepta in *mib*^{ta52b} mutant embryos is indistinguishable from that of wild type. This suggests that the initial cues responsible for patterning these vessels are normal and that a later step during pathfinding is likely affected. As mentioned previously, these vessel sprouts fail to express *ephrin-B2a* (Lawson *et al.*, 2001), which likely contributes to their improper targeting behavior, a phenotype also observed in mice lacking ephrin-B2 (Wang *et al.*, 1998).

As mentioned above, the analysis of head vessel structure in *mib*^{ta52b} mutant embryos could not be performed by using techniques such as confocal microangigraphy. Using the *TG(fli1:EGFP)*^{y1} transgenic line, we are now able to visualize the cranial vasculature *mib*^{ta52b} mutant embryos. We find that cranial vessels within the hindbrain are massively disorganized, appearing as a network of enlarged anastomotic sinuses rather than a stereotypical network of discrete interconnected vessels. Blood vessels such as the midcerebral vein that are located anterior to this region do appear to maintain normal patterning, but are much more dilated than in wild type siblings. Therefore, it is likely that these two major defects contribute to the severe cranial hemorrhage evident in *mib*^{ta52b} mutant embryos (Lawson *et al.*, 2001).

Although much of the early work that laid the foundation for studies of embryonic vascular development relied on simple observations using light microscopy, most subsequent work has utilized techniques that do not allow uninterrupted temporal observation of these processes *in vivo*. Organisms such as the mouse have definitively confirmed the functional importance of many of the molecules required for vascular development, although detailed analysis of mutant vascular phenotypes is often difficult due to the internal development of mammalian embryos. The zebrafish has proven to be an ideal tool for direct *in vivo* observations of developmental processes since its embryos develop externally, are transparent, and can be easily manipulated. The ability to visualize vascular development as it occurs *in vivo* in both wild type and mutant *TG(fli1:EGFP)* embryos makes the zebrafish a valuable tool for analyzing the cellular mechanisms that contribute to the formation of the vertebrate vasculature and will aid in the further identification of the molecular determinants that govern these processes.

ACKNOWLEDGMENTS

We thank Micheal Kacergis and Elizabeth Laver for access to *mind-bomb* and *albino* mutant carriers, respectively, and Van

Pham for helpful technical assistance. We gratefully acknowledge Jonathan Epstein for help in constructing the Web site associated with this article. We also thank Mark Williams for superb fish care and handling. Finally, we thank Sam Tesfai for assisting us with various aspects of multiphoton laser scanning microscopy.

REFERENCES

Adams, R. H., Wilkinson, G. A., Weiss, C., Diella, F., Gale, N. W., Deutsch, U., Risau, W., and Klein, R. (1999). Roles of ephrinB ligands and EphB receptors in cardiovascular development: Demarcation of arterial/venous domains, vascular morphogenesis, and sprouting angiogenesis. *Genes Dev.* **13,** 295–306.

Avraham, H., Cowley, S., Chi, S. Y., Jiang, S., and Groopman, J. E. (1993). Characterization of adhesive interactions between human endothelial cells and megakaryocytes. *J. Clin. Invest.* **91,** 2378–2384.

Bray, D., and Chapman, K. (1985). Analysis of microspike movements on the neuronal growth cone. *J. Neurosci.* **5,** 3204–3213.

Chien, C. B., Rosenthal, D. E., Harris, W. A., and Holt, C. E. (1993). Navigational errors made by growth cones without filopodia in the embryonic Xenopus brain. *Neuron* **11,** 237–251.

Clark, E. R. (1918). Studies on the growth of blood vessels in the tail of the frog larvae. *Am. J. Anat.* **23,** 37–88.

Cleaver, O., and Krieg, P. A. (1999). Molecular mechanisms of vascular development. In "Heart Development" (R. P. Harvey and N. Rosenthal, Eds.), pp. 221–252. Academic Press, San Diego.

Coffin, J. D., and Poole, T. J. (1988). Embryonic vascular development: Immunohistochemical identification of the origin and subsequent morphogenesis of the major vessel primordia in quail embryos. *Development* **102,** 735–748.

Denk, W., and Svoboda, K. (1997). Photon upmanship: why multiphoton imaging is more than a gimmick. *Neuron* **18,** 351–357.

Djonov, V., Schmid, M., Tschanz, S. A., and Burri, P. H. (2000). Intussusceptive angiogenesis: Its role in embryonic vascular network formation. *Circ. Res.* **86,** 286–292.

Gerety, S. S., Wang, H. U., Chen, Z. F., and Anderson, D. J. (1999). Symmetrical mutant phenotypes of the receptor EphB4 and its specific transmembrane ligand ephrin-B2 in cardiovascular development. *Mol. Cell* **4,** 403–414.

Gray, H. (1901). "Gray's Anatomy." Running Press, Philadelphia.

Hauptmann, G., and Gerster, T. (1994). Two-color whole-mount in situ hybridization to vertebrate and Drosophila embryos. *Trends Genet.* **10,** 266.

Helbling, P. M., Saulnier, D. M., and Brandli, A. W. (2000). The receptor tyrosine kinase EphB4 and ephrin-B ligands restrict angiogenic growth of embryonic veins in *Xenopus laevis*. *Development* **127,** 269–278.

Herbomel, P., Thisse, B., and Thisse, C. (1999). Ontogeny and behaviour of early macrophages in the zebrafish embryo. *Development* **126,** 3735–3745.

Hirakow, R., and Hiruma, T. (1981). Scanning electron microscopic study on the development of primitive blood vessels in chick embryos at the early somite-stage. *Anat. Embryol.* **163,** 299–306.

Isogai, S., Horiguchi, M., and Weinstein, B. M. (2001). The vascular anatomy of the developing zebrafish: An atlas of embryonic and early larval development. *Dev. Biol.* **230,** 278–301.

Jiang, Y. J., Brand, M., Heisenberg, C. P., Beuchle, D., Furutani-Seiki, M., Kelsh, R. N., Warga, R. M., Granato, M., Haffter, P., Hammerschmidt, M., Kane, D. A., Mullins, M. C., Odenthal, J., van Eeden, F. J., and Nusslein-Volhard, C. (1996). Mutations affecting neurogenesis and brain morphology in the zebrafish, *Danio rerio*. *Development.* **123,** 205–216.

Kimmel, C. B., Ballard, W. W., Kimmel, S. R., Ullmann, B., and Schilling, T. F. (1995). Stages of embryonic development of the zebrafish. *Dev. Dyn.* **203,** 253–310.

Latker, C. H., Feinberg, R. N., and Beebe, D. C. (1986). Localized vascular regression during limb morphogenesis in the chicken embryo. II. Morphological changes in the vasculature. *Anat. Rec.* **214,** 410–417, 392–393.

Lawson, N. D., Scheer, N., Pham, V., Kim, C.-H., Chitnis, A. B., Campos-Ortega, J., and Weinstein, B. M. (2001). Notch signaling is required for arterial-venous differentiation during embryonic vascular development. *Development* **128,** 3675–3683.

Lin, S. (2000). Transgenic zebrafish. *Methods Mol. Biol.* **136,** 375–383.

Mager, A. M., Grapin-Botton, A., Ladjali, K., Meyer, D., Wolff, C. M., Stiegler, P., Bonnin, M. A., and Remy, P. (1998). The avian fli gene is specifically expressed during embryogenesis in a subset of neural crest cells giving rise to mesenchyme. *Int. J. Dev. Biol.* **42,** 561–572.

Marin-Padilla, M. (1985). Early vascularization of the embryonic cerebral cortex: Golgi and electron microscopic studies. *J. Comp. Neurol.* **241,** 237–249.

Meier, S. (1980). Development of the chick embryo mesoblast: Pronephros, lateral plate, and early vasculature. *J. Embryol. Exp. Morphol.* **55,** 291–306.

Melet, F., Motro, B., Rossi, D. J., Zhang, L., and Bernstein, A. (1996). Generation of a novel Fli-1 protein by gene targeting leads to a defect in thymus development and a delay in Friend virus-induced erythroleukemia. *Mol. Cell. Biol.* **16,** 2708–2718.

Meyer, D., Wolff, C. M., Stiegler, P., Senan, F., Befort, N., Befort, J. J., and Remy, P. (1993). XI-fli, the Xenopus homologue of the fli-I gene, is expressed during embryogenesis in a restricted pattern evocative of neural crest cell distribution. *Mech. Dev.* **44,** 109–121.

Motoike, T., Loughna, S., Perens, E., Roman, B. L., Liao, W., Chau, T. C., Richardson, C. D., Kawate, T., Kuno, J., Weinstein, B. M., Stainier, D. Y., and Sato, T. N. (2000). Universal GFP reporter for the study of vascular development. *Genesis* **28,** 75–81.

Nilsen, N. O. (1981). Microangiography in explanted chick embryos. *Microvasc. Res.* **22,** 156–170.

Pardanaud, L., Altmann, C., Kitos, P., Dieterlen-Lievre, F., and Buck, C. A. (1987). Vasculogenesis in the early quail blastodisc as studied with a monoclonal antibody recognizing endothelial cells. *Development* **100,** 339–349.

Pardanaud, L., Yassine, F., and Dieterlen-Lievre, F. (1989). Relationship between vasculogenesis, angiogenesis and haemopoiesis during avian ontogeny. *Development* **105,** 473–485.

Poole, T. J., and Coffin, J. D. (1989). Vasculogenesis and angiogenesis: Two distinct morphogenetic mechanisms establish embryonic vascular pattern. *J. Exp. Zool.* **251,** 224–231.

Risau, W., and Flamme, I. (1995). Vasculogenesis. *Annu. Rev. Cell Dev. Biol.* **11,** 73–91.

Sabin, F. (1920). Studies on the origin of blood-vessels and of red blood corpuscles as seen in the living blastoderm of chicks on the second day of incubation. *Contrib. Embryol.* **36,** 213–261.

Streisinger, G., Singer, F., Walker, C., Knauber, D., and Dower, N. (1986). Segregation analyses and gene-centromere distances in zebrafish. *Genetics* **112,** 311–319.

Thompson, M. A., Ransom, D. G., Pratt, S. J., MacLennan, H., Kieran, M. W., Detrich, H. W., 3rd, Vail, B., Huber, T. L., Paw, B., Brownlie, A. J., Oates, A. C., Fritz, A., Gates, M. A., Amores, A., Bahary, N.,

Talbot, W. S., Her, H., Beier, D. R., Postlethwait, J. H., and Zon, L. I. (1998). The cloche and spadetail genes differentially affect hematopoiesis and vasculogenesis. *Dev. Biol.* **197,** 248–269.

Wagner, R. C. (1980). Endothelial cell embryology and growth. *Adv. Microcirc.* **9,** 45–75.

Wang, H. U., Chen, Z. F., and Anderson, D. J. (1998). Molecular distinction and angiogenic interaction between embryonic arteries and veins revealed by ephrin-B2 and its receptor Eph-B4. *Cell* **93,** 741–753.

Weinstein, B. M., Stemple, D. L., Driever, W., and Fishman, M. C. (1995). Gridlock, a localized heritable vascular patterning defect in the zebrafish. *Nat. Med.* **1,** 1143–1147.

Westerfield, M. (1993). "The Zebrafish Book." Univ. of Oregon Press, Eugene,1 OR.

Xu, Q. (1999). Microinjection into zebrafish embryos. In "Molecular Methods in Developmental Biology" (M. Guille, Ed.), Vol. 127, pp. 125–132. Humana Press, Inc., Totowa, NJ.

Zhou, R. (1998). The Eph family receptors and ligands. *Pharmacol. Ther.* **77,** 151–181.

Received for publication January 23, 2002
Revised April 4, 2002
Accepted April 24, 2002
Published online July 9, 2002